Upconversion photoluminescence by charge transfer in a van der Waals trilayer

Shengcai Hao, 1,2 Dawei He,1 Qing Miao,1 Xiuxiu Han,1 Shuangyan Liu,1 Yongsheng

Wang.^{1, a)} and Hui Zhao^{2, b)}

¹⁾Key Laboratory of Luminescence and Optical Information, Ministry of Education,

Institute of Optoelectronic Technology, Beijing Jiaotong University, Beijing 100044,

China

²⁾Department of Physics and Astronomy, The University of Kansas, Lawrence,

Kansas 66045, United States

(Dated: 23 September 2019)

As an elementary process of light-matter interaction in solids, upconversion photolumines-

cence has been extensively studied in rare-earth-doped materials and found applications in

biological imaging, infrared light detection, and laser cooling. More recently, it has been

shown that upconversion photoluminescence can be achieved in two-dimensional semicon-

ductors by utilizing the strong coupling between charge carriers. Here we show that the in-

terlayer charge transfer, which has been widely observed in van der Waals heterostructures,

can be utilized for upconversion photoluminescence. Using a MoSe₂/WS₂/MoS₂ trilayer

as an example, we show that by exciting the MoSe₂ and MoS₂ layers with a low-energy

670-nm laser beam, photoluminescence of 620 nm can be obtained. The upconversion pho-

toluminescence originates from the transfer of electrons and holes from MoSe₂ and MoS₂,

respectively, to the middle WS2 layer, where they recombine. The results illustrate an un-

explored physical mechanism for upconversion photoluminescence in solids and introduce

van der Waals heterostructures as materials to achieve upconversion photoluminescence.

1

a) Electronic mail: yshwang@bjtu.edu.cn

b)Electronic mail: huizhao@ku.edu

In a photoluminescence (PL) process, excitation photons produce photocarriers in forms of free electron-hole pairs or excitons. Typically, these photocarriers lose part of their energy to lattice or defects before their radiative recombination. As a result, the emitted photons have less energy than the excitation photons and the PL processes are known as Stokes processes. In some special situations, however, the photocarriers can gain energy and thus emit more energetic photons when they recombine. This anti-Stokes process is known as upconversion PL. Previously, upconversion PL has been mostly observed and studied in rare-earth-doped materials with the upconversion achieved *via* different energy levels of the rare-earth atoms^{1–6}. Such materials can be utilized in biological imaging^{7–10}, infrared detection^{11–15}, optical refrigeration^{16–18}, force sensors¹⁹, and photovoltaics²⁰.

The recently discovered two-dimensional (2D) materials, such as transition metal dichalcogenides (TMDs), provide another platform to explore upconversion PL. The reduced dielectric screening in such materials results in significantly enhanced Coulomb interaction between charge carriers, which enables formation of stable multicarrier complexes such as excitons, trions, and biexcitons. These quasiparticles with well-resolved inner electronic structures offer new physics mechanisms for upconversion PL. For example, upconversion from trion and exciton states has been observed in WSe₂²¹ and WS₂ monolayers²². In MoSe₂ monolayers embedded in photonic microstructures, conversion from the lower to upper polariton-trion states resulted in upconversion PL²³. Conversion from the lower-energy A-exciton states to the higher energy B-excitons states can offer upconversion PL with an energy of several hundreds of millielectrovolts²⁴. Furthermore, the upconversion PL spectroscopy has been used to study excited states in TMDs²⁵. In addition, there have been reports on upconversion PL from other 2D-related structures, such as defects in BN²⁶ and graphene quantum dots^{27–29}.

Here we report observation of upconversion PL in a 2D van der Waals heterostructure based on charge transfer. Using a MoSe₂/WS₂/MoS₂ trilayer as an example, we show that by properly designing the band alignment, it is possible to excite the layers with narrower bandgaps by low-energy photons and steer the excited carriers to the wider-gap layer, where they emit photons with an energy higher than the excitation energy. Our results introduce an unexplored mechanism for upconversion PL in solids and illustrate the potential of van der Waals heterostructures for upconversion PL applications.

We designed a trilayer van der Waals heterostructure where a wide-gap monolayer WS₂ is sandwiched by two monolayers with narrower bandgaps, MoSe₂ and MoS₂. Figure 1 shows the band

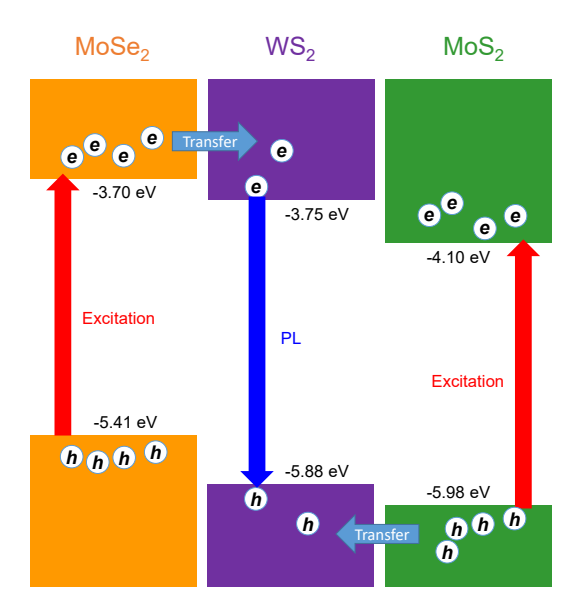


FIG. 1. The mechanism of upconversion photoluminescence in the van der Waals trilayer of $MoSe_2/WS_2/MoS_2$. Electrons (e) and holes (h) are excited in $MoSe_2$ and MoS_2 by low-energy photons. Due to the ladders band alignment in both the conduction and the valence bands, electrons in $MoSe_2$ and holes in MoS_2 transfer to WS_2 , where they recombine and emit photons with an energy equals to the optical bandgap of WS_2 that is larger than the excitation photons.

alignment of this trilayer, where the upper and lower boxes represent the conduction and valence bands of these monolayers, respectively. The numbers indicate the energy of the conduction band minimum and valence band maximum with respect to the vacuum level, according to theoretical results³⁰. The key elements of this design is that both the conduction and the valence bands of the three monolayers form a ladder structure and that the middle layer has the largest bandgap. When the sample is excited by photons (red vertical arrows) with an energy smaller than the WS₂ bandgap but larger than that of MoSe₂ and MoS₂, electrons (e) and holes (h) are excited in the left and right layers, as shown in Figure 1. The band alignment dictates that electrons will transfer from MoSe₂ to WS₂ and then MoSe₂. This makes it possible for some of the electrons and holes to meet in WS₂ and recombine, emitting photons (blue vertical arrow) with an energy equals to the WS₂ bandgap, and thus is higher than the excitation photon energy.

Figure 2(a) shows an optical microscopic image of the sample, which was fabricated by a mechanical exfoliation and dry transfer technique³¹. We first obtained monolayer flakes of MoSe₂, WS₂ and MoS₂ on polydimethylsiloxane (PDMS) substrates. Their monolayer thickness was iden-

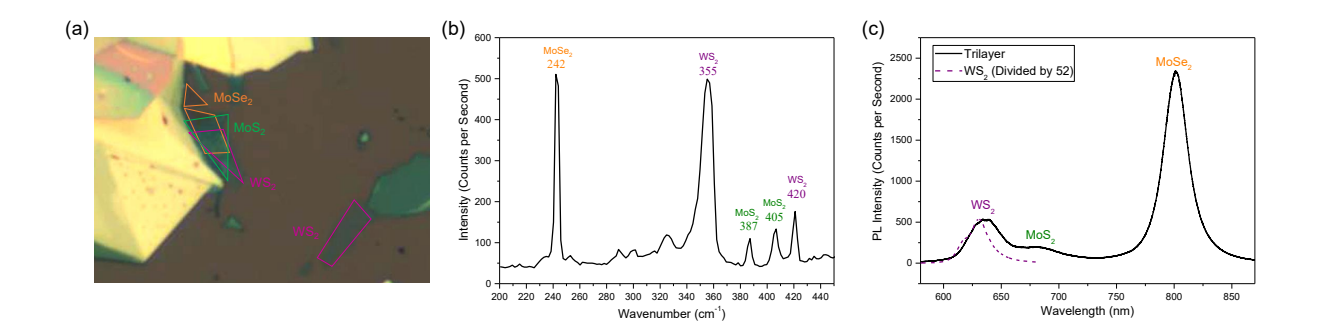


FIG. 2. (a) Optical microscopic image of the trilayer sample and a individual WS_2 monolayer. (b) Raman spectrum of the trilayer under 532-nm excitation. Raman peaks corresponding to each material are labeled in the figure. (c) Photoluminescence spectrum and the trilayer (solid black curve) and the WS_2 monolayer (dashed purple curve) under the same excitation condition of 532-nm and 0.4 mW.

tified by their optical contrasts³¹. The $MoSe_2$ flake was then transferred to a silicon substrate covered by a 90 nm thermal SiO_2 layer and was annealed for 2 h at $200^{\circ}C$ in a H_2/Ar (10 sccm /100 sccm) environment with a pressure of 2 Torr. Next, the WS_2 flake was transferred onto the $MoSe_2$ flake, followed by the same annealing procedure. Last, the MoS_2 flake was transferred onto the $MoSe_2/WS_2$ bilayer region, followed again by the annealing procedure under the same conditions. A separate WS_2 monolayer was also transferred near the trilayer to facilitate their comparison.

The sample was characterized by Raman and standard PL spectroscopic measurements. Figure 2(b) shows a Raman spectrum of the trilayer obtained by using a confocal Raman system, Horiba LabRAM HR Evolution, with a spectral resolution of 3 cm⁻¹. The excitation source is a 532-nm laser with an incident power of 0.4 mW. The Raman peaks correspond to each layer are labeled in the figure. The 242-cm⁻¹ peak is in excellent agreement with previous Raman measurements of monolayer MoSe₂³². For WS₂, the observed peaks at 355 and 420 cm⁻¹ are consistent with previously reported results³³. Finally, the Raman peaks at 387 and 405 cm⁻¹ with a separation of 18 cm⁻¹ agree well with results from monolayer MoS₂³⁴. These results further confirm the monolayer thickness of the three materials and their high quality after the transfer and annealing. Using the same spectrometer, we obtained the PL spectra of the trilayer and the WS₂ monolayer under the same excitation conditions, as shown in Figure 2(c). Peaks corresponding to the three materials are identified, as labeled in the figure. The peak from WS₂ is about 50 times weaker than the individual WS₂ monolayer. Such a PL quenching is a signature of efficient electron transfer between the atomic layers, which confirms the high interface quality of the sample^{35–39}.

The upconversion PL spectroscopic measurements were performed with a homemade micro-PL system based on a Horiba iHR550 imaging spectrometer equipped with a thermoelectrically cooled charge-coupled device camera. Two diode lasers with wavelengths of 670 and 785 nm are combined by a beamsplitter and are co-focused to the sample through a microscope objective lens. An imaging system was constructed to observe the sample and to locate the laser spot on the desired regions of the sample. The PL was collected in the reflection geometry.

Figure 3 summarizes a set of measurements that establish the upconversion PL of the trilayer. First, the black squares show the PL spectrum from the MoSe₂/WS₂/MoS₂ trilayer under the excitation of the 670-nm beam with a power of 10 μ W, with the 785-nm beam blocked. The PL observed at 620 nm is about 50 nm shorter than the excitation wavelength. The 670-nm beam is tuned to the optical bandgap of MoS₂ but is also capable of exciting MoSe₂, which has an optical bandgap of 785 nm. Hence, both MoS₂ and MoSe₂ layers are excited, as illustrated in Figure 1. The PL energy of 620-nm indicates that it is from recombination of excitons in WS₂. Since the WS₂ layer is not excited, the excitons in WS₂ are formed by electrons from MoSe₂ and holes from MoSe₂, as schematically shown as the horizontal arrows in Figure 1. The rather low PL counts could be attributed to the fact that WS₂ is an intermediate step of the ultrafast charge transfer process, and hence is only populated for an ultrashort period of time. For comparison, when the WS₂ layer of the trilayer sample was directly excited by a 405 nm laser beam, we observed a PL yield

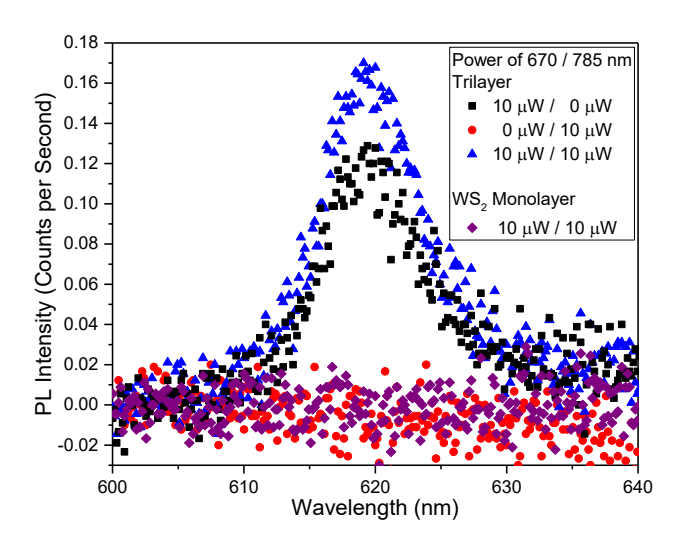


FIG. 3. Upconversion photoluminescence of MoSe₂/WS₂/MoS₂ trilayer under the excitation of 10 μ W of 670 nm (black squares), of 10 μ W of 785 nm (red circles), and of both the 10 μ W of 670 nm and the 10 μ W of 785 nm (blue triangles), as well as that of monolayer WS₂ excited by both beams.

that is about two orders of magnitude higher than the upconversion PL process.

To confirm this interpretation, we repeated the measurement by exciting the sample with $10 \mu W$ of 785-nm beam, with the 670-nm beam blocked. The red circles in Figure 3 show that no PL was detected. Since the 785-nm beam only excites MoSe₂, no holes are supplied to WS₂, and hence no exciton formation. We next used both beams to excite the sample together. The PL (blue triangles in Figure 3) is slightly increased from that excited by the 670-nm beam only. Finally, we move the WS₂ monolayer to the excitation region. Even with both beams present, no PL was detectable, as shown by the purple diamonds in Figure 3. The lack of signal from the individual WS₂ monolayer shows unambiguously the key role played by the other two layers, and thus strongly support our interpretation. This also rules out the possibility that the WS₂ layer were directly excited by, for example two-photon absorption of each beam or nondegenerate two-photon absorption of the two beams. If these direct-excitation processes were the origin, the PL of the individual WS₂ monolayer would have been about 50 times stronger than the trilayer, based on Figure 2(c).

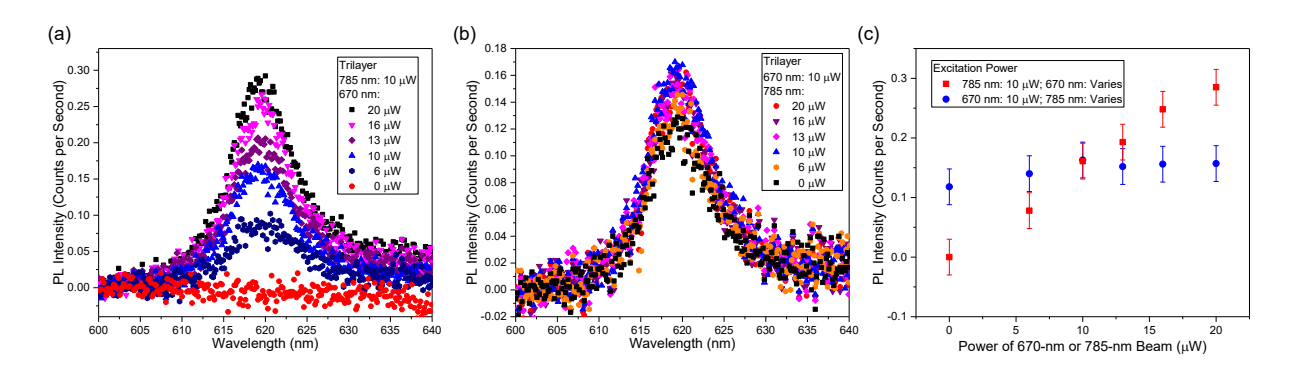


FIG. 4. Power dependence of the upconversion photoluminescence. (a) Photoluminescence spectra of the $MoSe_2/WS_2/MoS_2$ trilayer with a 785-nm excitation beam of 10 μ W and 670-nm beams with various powers as labeled. (b) Same as (a) but with the 785-nm power changes and the 670-nm power fixed at 10 μ W. (c) Peak photoluminescence of the trilayer as a function of either the 670-nm (red squares) or the 785-nm power (blue circles) obtained from (a) and (b).

We also studied the power dependence of the upconversion PL, as summarized in Figure 4. At first, we fixed the power of the 785-nm beam at 10 μ W and measure the PL spectra from the trilayer with various powers of the 670-nm beam. As shown in Figure 4(a), the upconversion PL increases with the 670-nm power. The red squares in Figure 4(c) show that the peak PL intensity increase nearly linearly with the 670-nm power. This feature is consistent with the mechanism

of the upconversion PL illustrated in Figure 1: Since the injected carrier densities in the MoSe₂ and MoS₂ layers are both proportional to the power, the additional carriers injected with a higher excitation power all participate the upconversion PL process. Next, we fixed the 670-nm power and studied how does the PL evolve with the power of the 785-nm beam. As shown in Figure 4(b) and the blue circles in Figure 4(c), the PL only slightly increases at low powers, and becomes nearly independent of the 785-nm power above 10 μ W. This feature can be attributed to the fact that the 785-nm beam only excites the MoSe₂ layer. Although the excited electrons can transfer to WS₂, holes stay in MoSe₂ and cannot contribute to the upconversion PL.

Recently, upconversion PL has been observed in TMD monolayers via higher-energy excitonic states, such as the B-exciton states and the excited states of A excitons of MoS_2^{21-25} . To rule out potential contributions from these states, some of which have similar energies of the A-excitons in WS_2^{40} , to the observed PL, we measured the region of MoS_2 monolayer under the excitation of 10 μ W of 670 and 785 nm. As shown by the gray squares in Figure 5, no PL was detected. If the upconversion PL observed from the trilayer (blue triangles) were from the excited states of MoS_2 , the PL intensity from MoS_2 monolayer would have been much higher than the trilayer due to the lack of charge-transfer-induced quenching. Similar measurement performed on the MoS_2/WS_2 bilayer region also produced no signal (orange circles in Figure 5). Furthermore, we

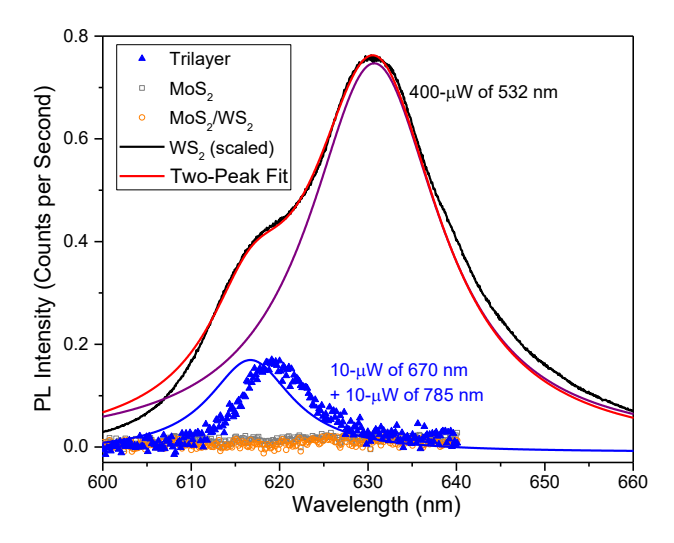


FIG. 5. Upconversion PL of MoSe₂/WS₂/MoS₂ trilayer (blue triangles, replotted from Figure 3), MoS₂ monolayer (gray squares), and MoS₂/WS₂ bilayer (orange circles) under the same excitation of 10 μ W of 670 nm and 10 μ W of 785 nm. The PL of WS₂ monolayer under 532-nm excitation is reploted from Figure 2 and decomposed to two peaks (blue and purple curves) for comparison.

decompose the PL spectrum of the WS_2 monolayer (black curve in Figure 5) to the sum of two components (red curve). The low-energy peak (purple curve) is due to the trion recombination, as previously identified⁴¹. The high-energy peak (blue curve) is from the A-excitons in WS_2 . The close similarity of the trilayer PL peak with this peak further confirms that the former is due to the A-excitons in the WS_2 layer, instead of excited excitonic states in MoS_2 . The small separation of the two peak is due to the different dielectric environments⁴² of the two WS_2 layers.

In summary, we have presented experimental evidence on an upconversion PL process in a van der Waals trilayer of MoSe₂/WS₂/MoS₂. By exciting the MoSe₂ and MoS₂ layers with a 670-nm beam, PL of 620 nm was observed. The upconversion PL was attributed to transfer of electrons and holes from MoSe₂ and MoS₂, respectively, to the middle WS₂ layer, where they recombine. This observation illustrates a charge-transfer-enabled physical mechanism for upconversion PL in solids, and introduces the 2D heterostructures to potential applications based on upconversion PL.

We are grateful for the financial support of the National Key R&D Program of China (2016 YFA0202302), the National Natural Science Foundation of China (61527817, 61875236), National Science Foundation of USA (DMR-1505852), and KU Research GO project.

REFERENCES

¹D. Matsuura, Appl. Phys. Lett. **81**, 4526 (2002).

²X. Qin, T. Yokomori, and Y. G. Ju, Appl. Phys. Lett. **90**, 073104 (2007).

³T. Aisaka, M. Fujii, and S. Hayashi, Appl. Phys. Lett. **92**, 132105 (2008).

⁴K. Suh, J. H. Shin, S. J. Seo, and B. S. Bae, Appl. Phys. Lett. **92**, 121910 (2008).

⁵J. Wang, R. R. Deng, M. A. MacDonald, B. L. Chen, J. K. Yuan, F. Wang, D. Z. Chi, T. S. A. Hor, P. Zhang, G. K. Liu, Y. Han, and X. Liu, Nat. Mater. **13**, 157 (2014).

⁶M. Y. Tse, M. K. Tsang, Y. T. Wong, Y. L. Chan, and J. H. Hao, Appl. Phys. Lett. **109**, 042903 (2016).

⁷J. Zhou, Z. Liu, and F. Y. Li, Chemi. Soc. Rev. **41**, 1323 (2012).

⁸Y. I. Park, K. T. Lee, Y. D. Suh, and T. Hyeon, Chem. Soc. Rev. **44**, 1302 (2015).

⁹R. Kumar, M. Nyk, T. Y. Ohulchanskyy, C. A. Flask, and P. N. Prasad, Adv. Funct. Mater. **19**, 853 (2009).

¹⁰Q. Q. Zhan, J. Qian, H. J. Liang, G. Somesfalean, D. Wang, S. L. He, Z. G. Zhang, and S. Andersson-Engels, ACS Nano 5, 3744 (2011).

- ¹¹G. Y. Chen, T. Y. Ohulchanskyy, R. Kumar, H. Agren, and P. N. Prasad, ACS Nano **4**, 3163 (2010).
- ¹²G. Y. Chen, T. Y. Ohulchanskyy, A. Kachynski, H. Agren, and P. N. Prasad, ACS Nano 5, 4981 (2011).
- ¹³J. Li, J. H. Zhang, Z. D. Hao, X. Zhang, J. H. Zhao, and Y. S. Luo, Appl. Phys. Lett. **101**, 121905 (2012).
- ¹⁴Q. C. Sun, H. Mundoor, J. C. Ribot, V. Singh, I. Smalyukh, and P. Nagpal, Nano Lett. **14**, 101 (2014).
- ¹⁵A. Das, C. C. Mao, S. Cho, K. Kim, and W. Park, Nat. Commun. **9**, 4828 (2018).
- ¹⁶R. I. Epstein, M. I. Buchwald, B. C. Edwards, T. R. Gosnell, and C. E. Mungan, Nature **377**, 500 (1995).
- ¹⁷J. Zhang, D. Li, R. Chen, and Q. Xiong, Nature **493**, 504 (2013).
- ¹⁸X. Zhou, B. E. Smith, P. B. Roder, and P. J. Pauzauskie, Adv. Mat. **28**, 8658 (2016).
- ¹⁹A. Lay, D. S. Wang, M. D. Wisser, R. D. Mehlenbacher, Y. Lin, M. B. Goodman, W. L. Mao, and J. A. Dionne, Nano Lett. **17**, 4172 (2017).
- ²⁰J. C. Goldschmidt and S. Fischer, Adv. Opt. Mater. **3**, 510 (2015).
- ²¹A. M. Jones, H. Y. Yu, J. R. Schaibley, J. Q. Yan, D. G. Mandrus, T. Taniguchi, K. Watanabe, H. Dery, W. Yao, and X. D. Xu, Nat. Phys. **12**, 323 (2016).
- ²²J. Jadczak, L. Bryja, J. Kutrowska-Girzycka, P. Kapuscinski, M. Bieniek, Y. S. Huang, and P. Hawrylak, Nat. Commun. **10**, 107 (2019).
- ²³N. Lundt, P. Nagler, A. Nalitov, S. Klembt, M. Wurdack, S. Stoll, T. H. Harder, S. Betzold, V. Baumann, A. V. Kavokin, C. Schuller, T. Korn, S. Hofling, and C. Schneider, 2D Mater. 4, 025096 (2017).
- ²⁴M. Manca, M. M. Glazov, C. Robert, F. Cadiz, T. Taniguchi, K. Watanabe, E. Courtade, T. Amand, P. Renucci, X. Marie, G. Wang, and B. Urbaszek, Nat. Commun. **8**, 14927 (2017).
- ²⁵B. Han, C. Robert, E. Courtade, M. Manca, S. Shree, T. Amand, P. Renucci, T. Taniguchi, K. Watanabe, X. Marie, L. E. Golub, M. M. Glazov, and B. Urbaszek, Phys. Rev. X 8, 031073 (2018).
- ²⁶Q. X. Wang, Q. Zhang, X. X. Zhao, X. Luo, C. P. Y. Wong, J. Y. Wang, D. Y. Wan, T. Venkatesan, S. J. Pennycook, K. P. Loh, G. Eda, and A. T. S. Wee, Nano Lett. 18, 6898 (2018).
- ²⁷M. Li, W. B. Wu, W. C. Ren, H. M. Cheng, N. J. Tang, W. Zhong, and Y. W. Du, Appl. Phys. Lett. **101**, 103107 (2012).

- ²⁸Q. Feng, Q. Q. Cao, M. Li, F. C. Liu, N. J. Tang, and Y. W. Du, Appl. Phys. Lett. **102**, 013111 (2013).
- ²⁹J. H. Shen, Y. H. Zhu, C. Chen, X. L. Yang, and C. Z. Li, Chem. Comm. **47**, 2580 (2011).
- ³⁰Y. Z. Guo and J. Robertson, Appl. Phys. Lett. **108**, 233104 (2016).
- ³¹F. Ceballos, P. Zereshki, and H. Zhao, Phys. Rev. Mater. 1, 044001 (2017).
- ³²S. Tongay, J. Zhou, C. Ataca, K. Lo, T. S. Matthews, J. B. Li, J. C. Grossman, and J. Q. Wu, Nano Lett. **12**, 5576 (2012).
- ³³N. Peimyoo, J. Shang, W. Yang, Y. Wang, C. Cong, and T. Yu, Nano Res. **8**, 1210 (2015).
- ³⁴C. Lee, H. Yan, L. E. Brus, T. F. Heinz, J. Hone, and S. Ryu, ACS Nano **4**, 2695 (2010).
- ³⁵P. Rivera, J. R. Schaibley, A. M. Jones, J. S. Ross, S. Wu, G. Aivazian, P. Klement, K. Seyler, G. Clark, N. J. Ghimire, J. Yan, D. G. Mandrus, W. Yao, and X. Xu, Nat. Commun. 6, 6242 (2015).
- ³⁶H. Fang, C. Battaglia, C. Carraro, S. Nemsak, B. Ozdol, J. S. Kang, H. A. Bechtel, S. B. Desai, F. Kronast, A. A. Unal, G. Conti, C. Conlon, G. K. Palsson, M. C. Martin, A. M. Minor, C. S. Fadley, E. Yablonovitch, R. Maboudian, and A. Javey, Proc. Natl. Acad. Sci. U. S. A. 111, 6198 (2014).
- ³⁷C. H. Lee, G. H. Lee, A. M. van der Zande, W. Chen, Y. Li, M. Han, X. Cui, G. Arefe, C. Nuckolls, T. F. Heinz, J. Guo, J. Hone, and P. Kim, Nat. Nanotechnol. **9**, 676 (2014).
- ³⁸M. M. Furchi, A. Pospischil, F. Libisch, J. Burgdorfer, and T. Mueller, Nano Lett. **14**, 4785 (2014).
- ³⁹S. Tongay, W. Fan, J. Kang, J. Park, U. Koldemir, J. Suh, D. S. Narang, K. Liu, J. Ji, J. Li, R. Sinclair, and J. Wu, Nano Lett. **14**, 3185 (2014).
- ⁴⁰Y. Li, A. Chernikov, X. Zhang, A. Rigosi, H. M. Hill, A. M. van der Zande, D. A. Chenet, E.-M. Shih, J. Hone, and T. F. Heinz, Phys. Rev. B **90**, 205422 (2014).
- ⁴¹X. He, Z. H. Zhang, C. H. Zhang, Y. Yang, M. Hu, W. K. Ge, and X. X. Zhang, Appl. Phys. Lett. **113**, 013104 (2018).
- ⁴²A. Raja, A. Chaves, J. Yu, G. Arefe, H. M. Hill, A. F. Rigosi, T. C. Berkelbach, P. Nagler, C. Schuller, T. Korn, C. Nuckolls, J. Hone, L. E. Brus, T. F. Heinz, D. R. Reichman, and A. Chernikov, Nat. Commun. 8, 15251 (2017).